An Integrated Metric for Rapid and Equitable Emergency Rescue During Extreme Floods in Urban Environments

ABSTRACT

After catastrophic flooding, quick and effective rescue operations are crucial to minimizing harm to vulnerable communities. While much research focused on emergency response and evacuation, few studies addresses how overhead powerline obstructions impact rescue operations. Additionally, existing research on vulnerable communities often emphasizes long-term flood mitigation and recovery, but less so on immediate responses. To ensure rapid and equitable flood rescue operations, this study derives an integrated metric to quantify rescue demands that incorporate rescue efficiency, community flood severity, and social vulnerability. In detail, rescue efficiency is calculated by analyzing a network that captures the geospatial interdependencies between the residential buildings' road networks and overhead power lines; community flood severity is quantified as the percentage of building damage resulting from flood impacts; and social vulnerability is an integrated indication of key household composition factors (e.g., elders, single parents, and minorities). Based on this metric, a systematic step is designed to suggest the sequence of rescue operations and the strategies for distributing rescue resources. The applicability and feasibility of the proposed approach were demonstrated using lifeboat rescue operations in Manville, New Jersey during Hurricane Ida. This study calculates dynamic changes in rescue loads of all emergency facilities and then finds the optimal strategies for distributing lifeboats. The results highlight the significant impact of overhead power line obstructions on the optimal rescue resources distribution. Practically, the generated rescue sequence and rescue resources distribution are expected to help emergency response agencies perform effective and rapid rescue operations.

Keywords: emergency rescue; flood modeling; road network modeling; powerline obstruction; resource allocation.

1. INTRODUCTION

Under climate change, the frequency and intensity of extreme precipitation events are increasing locally, especially in north-eastern areas of United States [1]. Compared with coastal flooding induced by storm surge that can often be predicted days in advance, flooding induced by heavy precipitation can develop within minutes to hours and the exact locations and severity are hard to predict, meaning shorter response time, smaller spatial scales, and longer lasting time [2][3][4]. Besides, precipitation-induced flooding could lead to inappropriate self-evacuation due to underestimations of hazards of shallow but speedy water flow [5][6], which places considerable demands and requests for efficient emergency response. Unlike rural environments, urban environments are typically featured by dense populations, extensive infrastructure, and intricate urban topography. These increase the complexity of emergency response efforts because the large volume of people needing evacuation can lead to traffic congestion and delays; the interdependent infrastructure systems can cause cascading failure that exacerbates flood impacts; and the varying ground elevations and land coverages can pose various levels of damage to different communities.

Transportation systems act as an essential role for emergency evacuations and search and rescue. Flood impacts to transportation systems, such as eroded and undermined roadbeds, spawned debris, and high-water incidents, can lead to highway closure that hinders emergency response and rescue operations. To address this issue, a vast amount of research has focused on identifying flood damage to transportation systems and analyzing traffic accessibility caused by the damage. For example, natural language processing and image processing techniques have been applied to extract flood damage-related information (e.g., damage severities and damage types) from publicly available image and text information [7][8]. Other research has modeled the topology of transportation systems to understand infrastructure cascading failures and identify vulnerable components through network analysis and simulation [9] [10]. To further understand residents' traveling patterns during flooding, research studies have used Agent-Based Modeling (ABM) to simulate residents' evacuation to identify vulnerable areas [11][12] and used machine learning-based approaches to rapidly predict hurricane evacuation traffic flows [13].

While significant research efforts have been taken to support emergency evacuation and rescue, existing studies have often oversimplified urban environments. Of the most importance are overhead powerlines, which is a system of electrical wires, supported by poles or towers, used to transmit electrical power across long distances from power plants to homes, businesses, and other end users. Overhead powerlines can complicate emergency evacuations for several reasons. For instance, downed powerlines can cause electrocution and fire hazards, which makes it dangerous for evacuees and emergency responders to navigate the area. Fallen powerlines can obstruct roads and pathways, which limits routes for evacuation and causes traffic congestion and delays in reaching safe areas. During the emergency planning phase, ignoring the impact of overhead powerlines' obstruction on emergency response activities could lead to biased decision-making [14], including unreliable estimations of road accessibilities, incorrect assumptions about the availability of rescue services, and unbalanced allocation of rescue resources.

Besides the availability of emergency services, social equity also plays a crucial role in emergency response activities because socially vulnerable households (e.g., elders and single-family households) are often exposed to greater risks and are less capable to safely evacuate by themselves. For example, elderly individuals and those with chronic health conditions often need specific evacuation assistance and low-income households may lack access to private transportation, making it difficult to evacuate independently. Although the importance of focusing on vulnerable communities during emergency evacuation and rescue is widely aware [15], existing studies that have considered social aspects are more oriented toward long-term flood mitigation, recovery, and rebuilding [16] [17] [4]. A few studies have considered social vulnerability during short-term emergency response; however, these studies have mainly focused on impassible road sections caused by flood and have not integrated the obstruction caused by overhead powerlines [18][19][20].

To address these research challenges, this study aims to answer one key question: how the obstruction of overhead powerlines and the consideration of socially vulnerable households impact the efficiency of emergency response planning and execution. In this study, 'emergency response' refers specifically to lifeboat-based rescue operations. Considering powerlines' obstruction on emergency response activities, the overhead powerlines in this manuscript refer to the lowest powerlines and the communication lines. The present study first employed an emergency response framework [14][21] to simulate the time-varied rescue routes during flooding expansion. Then an integrated metric considering flood hazards, rescue efficiency, and household composition is designed to quantify rescue demands for rescue operation prioritization at the census block level. Based on this metric, a systematic step is designed to suggest the sequence of rescue operations and the strategies for distributing rescue resources. To demonstrate the applicability and feasibility of the proposed approach, a case study in Manville, New Jersey following the impacts of Hurricane Ida was conducted. Specifically, the rescue demands at each time step are calculated and comparisons of the overall rescue loads on all emergency response facilities are made.

The remaining sections are organized as follows. The methodology section first describes the compositions of the integrated metric and then explains the mathematical details of the rescue demands quantification as well as the logic of rescue resource allocations. In the end, a discussion of the study findings and research contribution and limitations are summarized.

2. METHODOLOGY

The presented methodology is composed of four parts, data preparation, data pre-processing, integrated metric calculation, and rescue load calculation. In this section, the calculation of the integrated metric, which incorporates rescue efficiency, community flood severity, and social vulnerability is first introduced to quantify rescue demands. Based on this metric, a systematic step is designed to suggest the sequence of rescue operations and the strategies for distributing rescue resources. An illustration of the research methodology is shown in Figure 1.

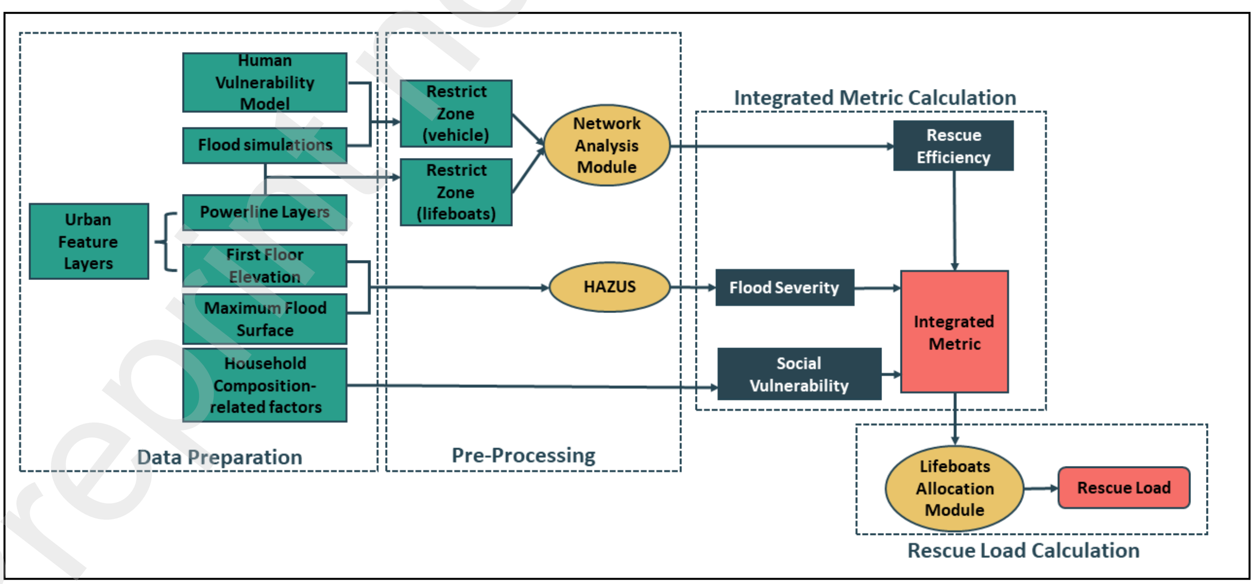

Figure 1. Research methodology flow chart.

2.1 Dynamic Rescue Demand Quantification

During and immediately after heavy rainfall, water levels rise rapidly, which can cause flash flooding with little warning. Once the water level remains stable, emergency rescue operations are carried out. To access the impacted residential buildings, emergency responders will dispatch lifeboats to pass the flooded road sections and deploy vehicles to pass the unaffected road sections. Considering obstructions of overhead powerlines, the flooded road sections that have geospatial dependency with powerlines which are previously passible would become impassible because of the proximity of rising floodwaters to the overhead powerlines. As water levels gradually recede, the status of road accessibility changes because some of the road sections that were previously not accessible by rescue boats or cars would become accessible. As a result, the time-varying characteristics of road accessibility would change and consequently impact the rescue demands. In this study, an integrated metric is designed to quantify rescue demands at various time steps for rescue operation prioritization. This metric considers three key aspects: the ability of responders travelling from emergency facilities to impacted households; the extent to which the buildings are destroyed by flood impacts; and the ability of households to safely evacuate to essential facilities. These aspects are indicated using rescue efficiency, community flood severity, and social vulnerability. A detailed explanation of each of these parts is given below.

2.1.1 Rescue efficiency

Rescue efficiency is defined as how fast emergency responders can travel from their emergency facility (i.e., shelters, fire stations, and emergency operation centers) to the flooded residential buildings. To consider the dynamic characteristics of road accessibility, an attributed road network is modeled to calculate rescue efficiency. Specifically, topological road attributes (road sections and road intersections) and building locations (i.e., emergency facilities and residential houses) are used to create an attributed network in which the nodes represent locations of emergency facilities, flooded residential buildings, road sections, and road intersections, and edges represent connections between road sections and connections between buildings and road sections. Three attributes are assigned to road sections and intersections: accessible by cars, accessible by boats, and not accessible by boats. These attributes are dynamically updated considering the flood depth and overhead powerline obstruction. If a road section/intersection becomes flooded and is not accessible due to overhead powerline obstruction, this node and its adjacent edges are removed from the network. An illustration of the dynamic process is illustrated in Figure 2. As flood recedes, the status of the highlighted road section changes (indicated in orange color) from not accessible by boats to accessible by boats and accessible by cars. The bottom part shows the disrupted road networks.

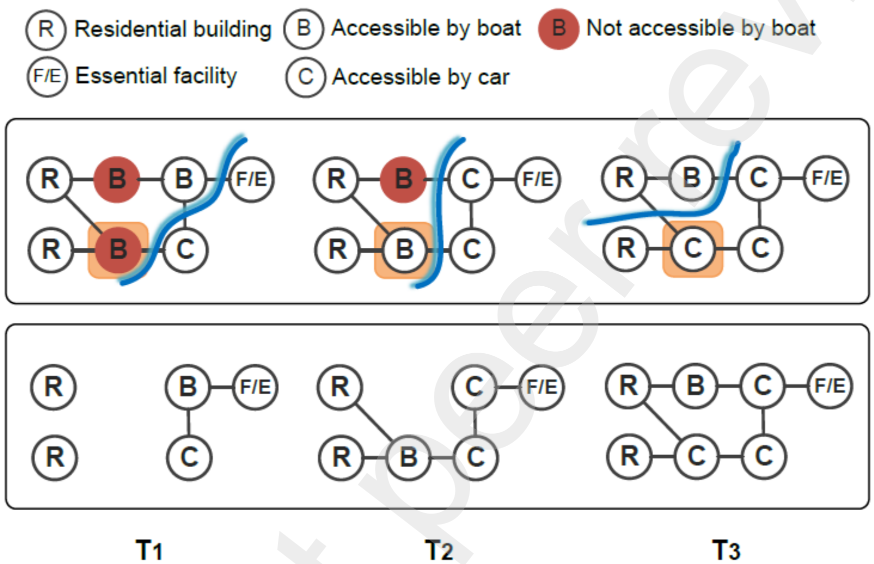

Figure 2. Illustration of the dynamic changes of road networks

The rescue efficiency (RE) is quantified as the inverse of the shortest path from an emergency facility to a flooded residential building. Mathematically, given a disrupted network G_t at timestep t, RE is formulated in Equation 1.

$$RE(G_t) = \frac{1}{d_{qn_t}} \quad t \in 1,2,\ldots,T \ \#(1)$$

Where q represents the emergency facility, n represents the flooded residential building, and d represents the shortest path from the emergency facility to the flooded residential buildings. The greater the rescue efficiency, the faster the emergency responders can reach the flooded building, and RE is dynamically updated given the latest road conditions.

2.1.2 Community flood severity

During emergency rescue, the extent to which a building is damaged influence rescue demands. The reason is that buildings that are more damaged by floods are at a higher risk of collapse. This poses an immediate threat to residents still living inside, making it urgent to rescue them before further deterioration occurs. Considering this effect, community flood severity is quantified as the percentage of flood-induced building damage. Due to the unique characteristics of building design attributes (e.g., presence of basement, first floor elevation, and construction materials), even with the same flood elevation, the extent of building damage would vary significantly. To derive the percentage of building damage, HAZUS—a GIS-based software developed by the Federal Emergency Management Agency (FEMA) to identify areas with high risk for natural hazards and estimate the physical, economic, and social impacts of hazards—is employed [22]. HAZUS can be used to estimate the damage percentage to individual buildings based on building inventory data and water depths. In detail, HAZUS employs depth-damage curves, which relate the depth of flooding to the percentage of damage for different types of buildings and are derived based on empirical data and engineering studies. Given the building design attributes and flood depth near each building, the percentage of structural damage is estimated based on the building's construction type and flood depth. The greater the percentage of building damage (PB), the more urgent it is to rescue residents living inside these buildings. It is worth noting that the depth-damage curve can also be manually specified using historical data. This often led to a more accurate building damage estimation. However, when such data are not available, HAZUS can be used as a convenient tool for general estimation. During flood impacts, since a building is less likely to become restored, the percentage of building damage is computed based on the maximum simulated flood depth and it is not affected by time.

2.1.3 Social vulnerability

Focusing on vulnerable households during emergency evacuation and rescue is critical because these groups are often exposed to greater risks and face more barriers to evacuate to safety. Socially vulnerable households, such as elders, single parents, and minorities, are less prepared for flood disruptions and need the most support, as a result, their rescue demands need prioritization. In the context of emergency evacuation, household composition is a key aspect that influences community evacuation ability. For example, households with children, elderly members, or individuals with disabilities have unique needs that can complicate evacuation. In this study, four household composition-related factors are selected: the percentage of persons aged 65 and older ($P_{65older}$), the percentage of persons aged 18 and younger ($P_{18younger}$), the percentage of minority households ($P_{miority}$), and the percentage of single-family households ($P_{singlefamily}$). Due to privacy concerns, identifying these four factors at the building level is not possible. As an alternative, census block data, which is the smallest unit of public data collected by the U.S. Census Bureau can be used [23]. To integrate the four factors, a percentile ranking approach is used. Specifically, each of the four variables is first ranked from the highest to lowest across all census blocks in the investigated community, where a higher ranking indicates a more vulnerable census block. Then, a percentile rank was calculated for each census block over these variables. In the end, the percentile ranks were summed to indicate a block's vulnerability to evacuate. By prioritizing census blocks that have higher rankings, emergency responders can ensure that vulnerable communities are not disproportionately affected by emergencies and that everyone has the opportunity to evacuate safely and receive the necessary support.

2.1.4 Rescue demands

The rescue demand is defined as a metric that integrates rescue efficiency, community flood severity, and social vulnerability introduced above, and it is used to inform emergency rescue at the census block level. Since rescue efficiency and community flood severity are derived at the building level, these metrics are first averaged at the blocked level. For a census block k with n number of residential buildings, the block-level rescue efficiency ($RE_{k,t}$) at a time step t is shown as follows:

$$RE_{k,t} = \frac{\sum_{N=1}^{n} \frac{1}{d_{qn_t}}}{n} \; k \in 1,2,\ldots,m, t \in 1,2,\ldots,T\#(2)$$

The block-level flood severity is calculated as follows:

$$FS_k = \frac{\sum_{N=1}^{n} PB_n}{n} \; k \in 1,2,\ldots,m \; \#(3)$$

Given the block-level rescue efficiency $RE_{k,t}$, flood severity FS_k, and social vulnerability SV_k, the rescue demands of a census block k at timestep t is ($RD_{k,t}$) computed by first calculating the percentile rank of each variable across all census blocks in an investigated community. Here, flood severity and social vulnerability are ranked from the highest to the lowest because a higher value indicates a greater demand for rescue. On the contrary, rescue efficiency is ranked from the lowest to highest because a higher efficiency indicates better evacuation ability. In the end, the percentile ranks were summed up to calculate $RD_{k,t}$.

2.2 Rescue Resource Allocations

Lifeboats are commonly used for rescue in inundated areas during flooding and they are the resources that are mainly concerned in this study. During emergency evacuations and rescues, lifeboats are assigned to emergency facilities through a coordinated and systematic approach to ensure efficiency and safety. To evaluate how the obstruction of overhead powerlines and the consideration of socially vulnerable households impact the efficiency of emergency response planning and execution, four different lifeboat allocation strategies are designed for comparison. First, the 'equal plan', which evenly distributes lifeboats among available emergency response facilities. The second one is named as 'fixed plan 1'. It allocates lifeboats based on the ratio calculated by the number of accessible census blocks associated with each emergency facility to the total count of census blocks needing rescue. This means a facility with a higher count of accessible census blocks will be assigned with more lifeboats. This strategy requires a pre-understanding of the accessibility of buildings and blocks, considering overhead powerlines' obstruction. 'Fixed plan 2' follows a similar pattern as "Fixed plan 1" but considers the total number of associated blocks per facility regardless of the accessibility and rescue requirements. 'Fixed plan 3' uses the integrated metric, rescue demands, to inform lifeboat allocation. Similarly, a ratio is specified. The difference is that the ratio is calculated through the summation of rescue demands of all associated census blocks of each facility. A higher summation indicates that generally the associated accessible census blocks have higher vulnerability and longer travel distances to the facilities, signifying a greater need for lifeboats. The allocation ratios of four strategies are calculated based on the worst conditions during a flood event and will not change as time goes by.

To track rescue progress, two status flags are introduced at each time step: the inherit flag N_1 and the rescue flag N_2. Initially, for all census blocks that will be flooded, N_1 is set to 1, indicating that none of these blocks have been rescued. At every subsequent time step, N_1 is updated to 0 for blocks that have been rescued and this status is inherited to the next time step. The rescue flag N_2 reflects the accessibility and flood hazards of specific census blocks; it is set to 1 for blocks that will be flooded and are accessible at the current time step, and 0 otherwise. At each time step, a new metric $CM_{k,t}$, calculated based on Equation 4 for each census block. It determines the rescue necessity, feasibility and emergency of all census blocks at specific time step t. Then by ranking the metric, the census blocks with top-ranked metric will be rescued at time step t.

$$CM_{k,t} = N_{1,k,t} \cdot N_{2,k,t} \cdot RD_{k,t} \quad k \in 1,2,\ldots.m, t \in 1,2,\ldots T \ \#(4)$$

Where m is the number of impacted census blocks. The rescue load RL, defined as the sum of the new metric CM of all impacted census blocks during flooding (Equation 5), will be employed here to track the rescue progress of using different allocation strategies.

$$RL_t = \sum_{k}^{m} CM_{k,t}, \quad k \in 1,2,\ldots m, t \in 1,2,\ldots T \ \#(5)$$

Where T is the number of time steps.

3. CASE STUDY

Hurricane Ida, which made landfall in Louisiana on August 29, 2021, as a category 4 storm, brought extreme rainfall to the greater New York metropolitan area on the night of September 1, 2021. This extreme rainfall triggered numerous flash flooding warnings and emergencies. Manville is a borough in Somerset County located in central New Jersey. It is bounded by the Raritan River in the north, the Millstone River on the east, Royce Brook to the south, and Hillsborough Township on the west. Officials report that recurrent flooding problems are prevalent throughout Manville in areas proximate to the Raritan River and the Millstone River, mainly due to the fluvial or river flooding from the Raritan and Millstone Rivers [24]. From September 1st through September 3rd, 2021, Tropical Storm Ida moved through the state of New Jersey, causing high winds and heavy rainfall. The Raritan River crested at about 27.6 feet, the highest ever recorded (the previous highest being Hurricane Floyd with a crest of 27.1 feet in 1999) [25]. Over 100 houses in Manville were partially or completely submerged under floodwater.

To demonstrate the applicability and feasibility of the proposed approach, the case study analyzes the rescue conditions in Manville Township during Hurricane Ida. This section starts by introducing the details of the flood condition reconstruction and overhead powerline extraction in Manville. Then, steps taken to calculate the dynamic rescue demands are explained. After this, the rescue progresses following the proposed lifeboat allocation strategies are compared and the reasons leading to different patterns are discussed.

3.1 Data Processing

3.1.1 Flood Reconstruction

The flood conditions for hurricane Ida in this study were reconstructed by a street-scaled 2-dimentional hydrodynamic model [26], validated by measured high water marks. The model domain encompasses the Raritan River Basin area from Branchburg to Bound Brook Township, incorporating three major upstream freshwater inputs. The river bathymetry, integrated into the background terrain used by the model, has been enhanced based on the most recent bathymetry dataset created by Rutgers University [27]. Additionally, to accurately capture the impact of buildings on flood spreading, building footprints were converted to a raster dataset with a consistent building height of 10 meters and then merged onto the background terrain. A spatially varied resolution mesh was employed, featuring a 3-meter resolution in flood-prone street areas and a resolution ranging from 10 to 50 meters for the remainder of the domain. The original shallow water equations, Eulerian-Lagrangian Method (SWE-ELM), were employed for performing two-dimensional unsteady flow routing in this case study.

3.1.2 Overhead Powerline Extraction

The methodology for extracting overhead power lines from a citywide point cloud dataset involves several key steps to ensure accurate and useful data. Initially, a point cloud dataset was collected, which includes detailed spatial information of the target area. This dataset is rich with various urban features such as buildings, trees, and overhead power lines. The extraction process begins by digitizing these overhead power lines into 3D polylines using specialized software like VRMesh V11.8.1 and ArcGIS 10.8.1. In VRMesh, the point cloud data was processed to identify and highlight the power lines. This involves semi-automated procedures to extract the elevation and location information of the power lines. However, due to potential spatial discontinuities caused by obstructions like vegetation, the extracted data may be incomplete. To address this, spatial interpolation techniques in ArcGIS were applied. The digitized polylines were converted into polygons with a buffer distance to facilitate accurate interpolation. This process ensures a continuous and coherent dataset representing the overhead power lines. Finally, the elevation and location information of the extracted power lines were exported as raster layers to assess the clearance distances above potential floodwater levels at each time step, ensuring the safety and effectiveness of rescue operations during flood events [14].

3.1.3 Rescue Efficiency

Based on the road network (polylines) and building footprints (polygons) in Manville, a citywide network was generated using a series of ArcPy scripts to connect all residents and emergency facilities (Figure 3). Road nodes were created every 13.7 meters (45 feet) along the road segments and assigned the type “C” or “B” to represent the accessibility status of each node. “C” indicates accessible by vehicles, while “B” indicates accessible by lifeboats. All building footprints within the study area were converted to building nodes and assigned the type “R,” “E,” or “F,” “R,” represents normal residential and commercial buildings, “E” represents evacuation centers, and “F” represents fire stations, with both “E” and “F” nodes being emergency response facilities. Each building node was then linked to its nearest road node, representing the connection status between the two nodes in the network.

At each time step, the accessibility status of all nodes was adjusted based on flood progression. For example, road nodes in vulnerable areas, identified using the human instability model [28], will change from “C” to “B,” indicating that these nodes are no longer accessible by vehicles. The assumption here is that areas that cannot be accessed by walking also cannot be accessed by vehicles due to higher relative motion speeds and limited flexibility in floodwaters. Additionally, the clearance distance between the water elevation and overhead power lines was calculated at each time step to identify restricted zones for lifeboats due to overhead power line obstructions [14]. Paths within these restricted zones were removed at each step to indicate inaccessibility. As shown in Figure 3, on September 2nd, 2021, all road nodes in walking-restricted areas changed from “C” to “B,” and all paths covered by boat-restricted areas were removed. Three essential facilities are identified in Manville, and the rescue efficiency is determined based on the closest accessible facilities.

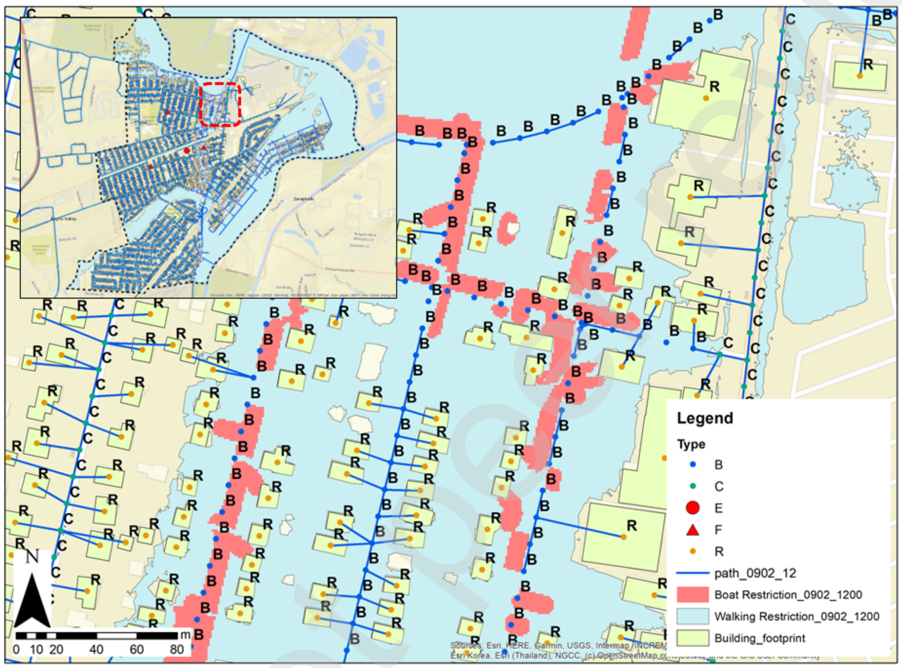

Figure 3. Example network accessibility on September 2nd, 2021 at 12:00 a.m.

Given the generated network at each timestep, the rescue efficiency for each census block at each hour is calculated following Equations (2).

3.1.4 Community Flood Severity

HAZUS was utilized to estimate the damage percentage to individual buildings using the processed building inventory data and the maximum water depth obtained from the flood reconstruction step (section 3.1.1). Here the building inventory data, such as the number of stories, roof type, exterior wall covering, and the presence of a basement, was processed by gathering data from njparcels.com and njpropertyrecords.com and surveying all the homes using Google Street View (GSV). One of the most important building attributes, first-floor elevation, a critical factor in determining a building's risk, was extracted from mobile LiDAR data collected by the Rutgers mobile mapping team following Hurricane Ida. Innovative technology, using Yolo5, a 2D object detector for identifying building components like windows, doors, and garage doors based on the intensity of the point cloud, is employed to extract the first-floor elevation [29]. Given the building damage percentage, Equation (3) is used to calculate community flood severity at each census block. An illustration of the building damage percentage for buildings that have damage percentages greater than zero is indicated in Figure 4. The graduated colors changing from white to blue represent the percentage of building damage, where a whiter color shows a low percentage of damage and darker blue shows a high percentage of damage.

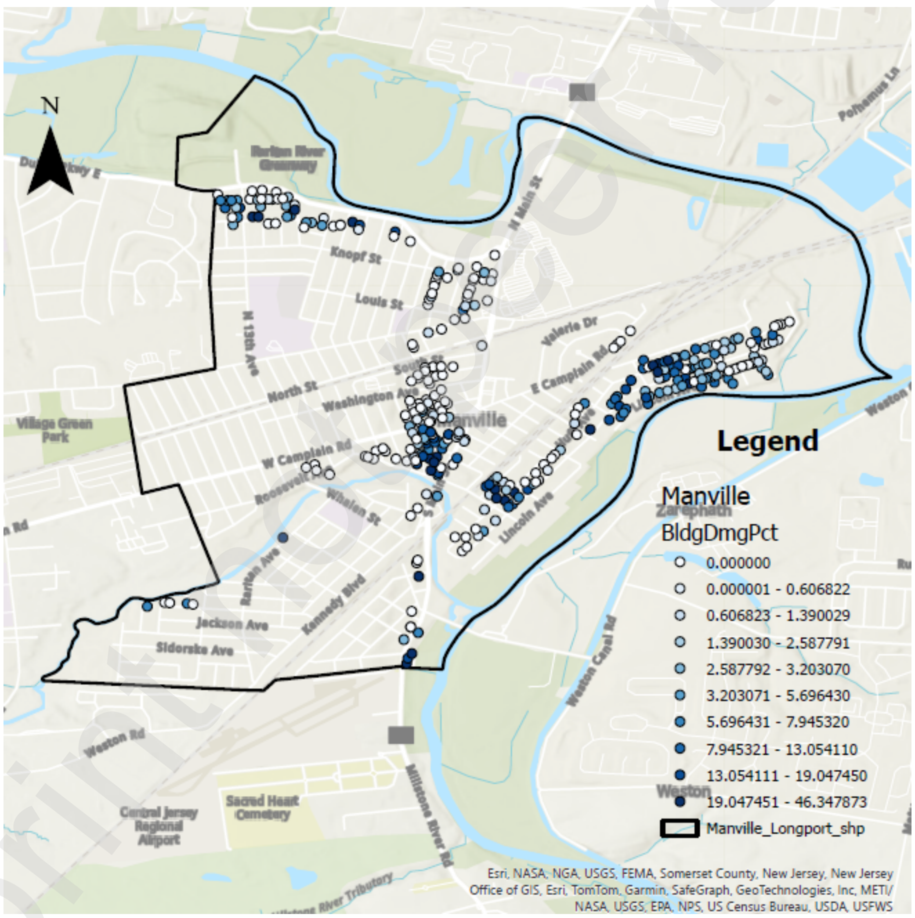

Figure 4. Percentage of building damage at Manville

3.1.5 Social Vulnerability and Integrated Metric

The block-level house composition data (i.e., the percentage of persons aged 65 and older, people aged 18 and younger in minority households, and single-family households) is obtained from the U.S.

Census Bureau [23]. Then following the proposed integrated metric calculation approach, the rescue demands of each census block at each hour were calculated. An illustration of the details of metric calculation process at one time step is shown in Table 1.

Block ID	Building Damage Percentage	Efficiency	Building Damage Percentage Percentile	Efficiency Percentile	SVI Percentile	Integrated Metric	Integrated Metric Percentile
1019514	0.095	0.007	0.943	0.912	0.866	0.907	1.000
1003514	0.110	0.009	0.964	0.809	0.892	0.888	0.995
1005514	0.097	0.009	0.948	0.825	0.887	0.887	0.990
1010514	0.052	0.006	0.907	1.000	0.716	0.875	0.985
...	...	...	...	...	...	...	...
1017515	0.000	0.056	0.327	0.052	0.196	0.192	0.021
2034516	0.000	0.041	0.327	0.108	0.093	0.176	0.015
2027516	0.000	0.100	0.327	0.010	0.098	0.145	0.010

Table 1. Illustration of the metric calculation process

The first column in Table 1 shows the block ID. For each block, the second and third columns show the building damage percentage and efficiency (derived in the rescue efficiency and flood severity sections) respectively. The fourth, fifth and sixth columns show the percentile ranks of building damage percentage, rescue efficiency, and social vulnerability index, across all census blocks. The integrated metric is calculated by averaging the three percentiles. In the end, a percentile ranking based on the integrated metric is derived to inform emergency rescue prioritization. At each time step, the percentile ranks are dynamically updated based on the latest road conditions.

3.2 Results

To compare and fully understand the performance of different allocation strategies, the rescue progresses under two scenarios are evaluated. These are rescue operations considering overhead powerline obstructions and neglecting overhead powerline obstructions. In the case study, the allocation ratios of lifeboats for four different allocation strategies were calculated, assuming the total available lifeboats for rescue operations is 6. The allocation ratio for the four strategies is [2,2,2] for the Equal Plan. [1,3,2] for Fixed Plan 1, [3,2,1] for Fixed Plan 2, and [2,3,1] for Fixed Plan 3. The current case study treats these allocation ratios to be constant and does not vary over time.

In this study, rescue operations are set to begin at the 13th time step, four hours after the peak level detected in the nearest river gage, initially under full rescue requirements. This assumption represents the worst-case scenario because the rescue loads are the highest. The changes in rescue loads under different scenarios are illustrated in Figure 5. The results found that the lifeboat allocation ('Fixed Plan 1') considering overhead power lines is the most effective strategy in both scenarios (see Figure 5), as it achieves the largest decrease rate in rescue load. When social vulnerability is considered ('Fixed Plan 3'), this strategy outperforms the equal allocation approach in scenarios without powerlines' obstruction in rescue activities, but it is less effective when powerlines' obstruction is considered. This is because of the imbalance between the total rescue demands and the number of census blocks with rescue needs, which will be further explained in the discussion section. The least effective strategy is 'Fixed Plan 2,' which does not account for rescue requests and accessibility; this outcome is not surprising since this approach is less targeted and lacks critical considerations. In scenarios where powerlines' obstruction is considered during rescue activities, the rescue load decreases before the start of rescue activities, as more blocks become inaccessible for lifeboats due to the proximity of rising floodwaters to the overhead powerlines. The increased rescue load after September 2nd at 23:00 is due to more blocks becoming accessible again as the water level recedes.

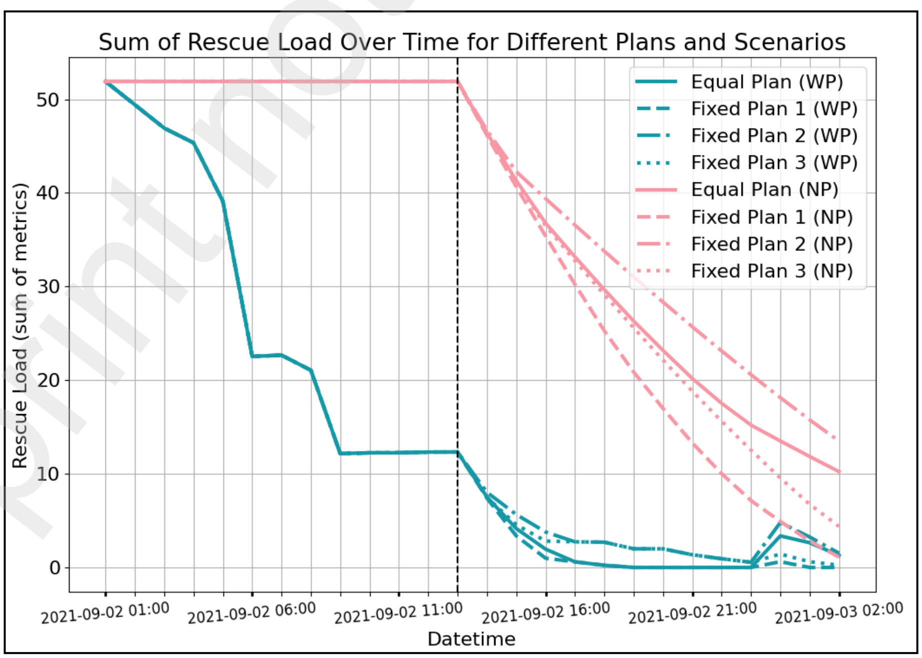

Figure 5 The rescue load variation using different lifeboat allocation strategies under two scenarios, rescue operations considering powerline obstruction or neglecting powerline obstruction. The left part of the black dash line indicates the rescue load before rescue activities. NP refers to 'No Powerlines Consideration Scenario', and WP refers to 'With Powerlines Consideration Scenario'

4. DISCUSSION

The allocation strategy based on the rescue requirement and accessibility status, i.e., Fixed Plan 1 is the most effective strategy because the distribution of rescue demands among emergency facilities is uneven in reality. Allocation plan without considering this uneven distribution will result in low effective rescue operations. For example, in this case study, facilities with the highest number of associated blocks often have a lower proportion of rescue demands during floods, and most associated census blocks are not impacted by flooding. Similarly, some facilities with fewer associated blocks but have a higher rescue demand because most of the associated census blocks are located in the flood-prone area. Interestingly, 'Fixed Plan 3', as a more considerable and targeted strategy, becomes less effective than Fixed Plan 2 no matter if the powerline obstruction is considered or not in rescue operations. 'Fixed Plan 3' is a strategy that allocates lifeboats based on the sum of integrated metrics of all associated census blocks to each emergency response facility. This means if the associated buildings are more vulnerable (higher sum of integrated metric), the facility will be assigned more lifeboats. However, being more vulnerable doesn't mean the number of required lifeboats will be higher. It is possible that the number of census blocks requiring rescue associated with one facility is high but with low social vulnerability in total. This will lead to one limitation of this study, which is the current analysis is based on static instead of dynamic allocation strategy, which means the allocation ratio among facilities will not change as time goes by. Lifeboats assigned to a facility with a higher vulnerable status but a lower number of census blocks that require rescue will be idle in the simulation, leading to a relatively low rescue efficiency overall. The future study will optimize the allocation strategy in a dynamic allocation way to ensure the available resources will be allocated precisely as demands. Additionally, future studies should broaden the study areas to develop a more generalized understanding of optimized allocation strategies taking powerline's obstruction into account. In particular, a better resource allocation strategy that considers the tradeoff between the block-level rescue demands and the actual number of households that require rescue is needed.

5. CONCLUSION

The unpredictable and localized nature of precipitation-induced flooding, together with the obstacles resulted from infrastructure damage and high-speed water flow, make emergency evacuation and rescue challenging. To help emergency responders carry out effective and rapid rescue operations, this research proposed an integrated metric to quantify the rescue demands at the census block level and designed a systematic step to simulate rescue operations using different lifeboat allocation strategies. The integrated metric considers rescue efficiency, community flood severity, and social vulnerability. These are defined as the ability of responders travelling from emergency facilities to impacted households; the extent to which the buildings are destroyed by flood impacts; and the ability of households to safely evacuate to essential facilities. The integrated metric (i.e., rescue demands) provides comprehensive guidance to prioritize rescue operations among census blocks. Following the systematic resource allocation strategies, the allocated lifeboats at emergency response facilities were calculated and then used to derive the rescue loads of the overall emergency rescue operation at each time step.

To demonstrate the applicability and feasibility of the proposed approach, a case study in Manville, New Jersey following the impacts of Hurricane Ida was conducted. Using the designed integrated metric and the resource allocation strategies, a comparison of rescue processing between two scenarios, considering or neglecting overhead power line impacts on lifeboat-based rescue operations during extreme flooding, was constructed to evaluate the impacts of overhead power line obstruction on emergency rescues. The results highlighted the significance of powerlines' obstruction should not be neglected for lifeboat allocation. The strategy considering overhead power line obstruction returns the highest decrease rate in rescue load in both scenarios. Furthermore, the differences among the rescue load variations in the two scenarios emphasize the need to account for powerline obstructions in simulations of emergency rescue during extreme flooding in urban environments.

Although it is expected that the resource allocation strategy that considers the proposed metric demonstrates the best performance, it is ranked as the second best-performing strategy. One possible reason is that the number of census blocks requiring rescue associated with one emergency facility is low, but the social vulnerability of these census blocks is high. Then the allocated lifeboats will be larger than the actual requirement. And the time-invariant allocation in this study leads to a waste of rescue resources in later periods of rescue. The future study will optimize the allocation strategy in a dynamic allocation way to ensure the available resources will be allocated precisely as demands. Additionally, future studies should broaden the study areas to develop a more generalized understanding of optimized allocation strategies taking powerline's obstruction into account.

ACKNOWLEDGEMENT

This material is based upon work supported by the U.S. National Science Foundation under award 2103754, by FEMA under HMGP DR4488. The views and conclusions contained in this document are those of the authors and should not be interpreted as necessarily representing the official policies, either expressed or implied, of the U.S. National Science Foundation and FEMA. The authors would like to thank Holly Joseph for sharing the building damage percentage data.

REFERENCE

[1] H. Tabari, "Climate change impact on flood and extreme precipitation increases with water availability," *Scientific Reports,* vol. 10, *(1),* pp. 13768, 2020. Available: https://doi.org/10.1038/s41598-020-70816-2. DOI: 10.1038/s41598-020-70816-2.

[2] J. Schanze, "Pluvial flood risk management: an evolving and specific field," *J Flood Risk Management,* vol. 11, *(3),* pp. 227-229, 2018. Available: https://doi.org/10.1111/jfr3.12487. DOI: 10.1111/jfr3.12487.

[3] C. Corral *et al*, "Comparison of two early warning systems for regional flash flood hazard forecasting," *Journal of Hydrology,* vol. 572, pp. 603-619, 2019. Available: https://www.sciencedirect.com/science/article/pii/S0022169419302665. DOI: 10.1016/j.jhydrol.2019.03.026.

[4] Y. Li, F. Zhang and W. Ji, "Integrated Data-Driven and Equity-Centered Framework for Highway Restoration Following Flood Inundation," *Journal of Management in Engineering,* vol. 39, *(3),* pp. 4023012, 2023.

[5] M. Shirvani, G. Kesserwani and P. Richmond, "Agent-based modelling of pedestrian responses during flood emergency: mobility behavioural rules and implications for flood risk analysis," *Journal of Hydroinformatics,* vol. 22, *(5),* pp. 1078-1092, 2020. Available: https://doi.org/10.2166/hydro.2020.031. DOI: 10.2166/hydro.2020.031.

[6] Y. Wang and R. Marsooli, "Physical Instability of Individuals Exposed to Storm-Induced Coastal Flooding: Vulnerability of New Yorkers During Hurricane Sandy," *Water Res.,* vol. 57, *(1),* pp. e2020WR028616, 2021. Available: https://doi.org/10.1029/2020WR028616. DOI: 10.1029/2020WR028616.

[7] C. Yudi, W. Qi and J. Wenying, "Rapid Assessment of Disaster Impacts on Highways Using Social Media," *J. Manage. Eng.,* vol. 36, *(5),* pp. 04020068, 2020. Available: https://doi.org/10.1061/(ASCE)ME.1943-5479.0000836. DOI: 10.1061/(ASCE)ME.1943-5479.0000836.

[8] H. Hao and Y. Wang, "Leveraging multimodal social media data for rapid disaster damage assessment," *International Journal of Disaster Risk Reduction,* vol. 51, pp. 101760, 2020. Available: https://www.sciencedirect.com/science/article/pii/S2212420920312620. DOI: 10.1016/j.ijdrr.2020.101760.

[9] I. Hernandez-Fajardo and L. Dueñas-Osorio, "Probabilistic study of cascading failures in complex interdependent lifeline systems," *Reliab. Eng. Syst. Saf.,* vol. 111, pp. 260-272, 2013. Available: https://www.sciencedirect.com/science/article/pii/S0951832012002153. DOI: 10.1016/j.ress.2012.10.012.

[10] Y. Li, F. Zhang and W. Ji, "Automated integration of infrastructure component status for real-time restoration progress control: Case study of highway system in hurricane harvey," in *Proceedings of the Winter Simulation Conference*Anonymous 2022, .

[11] D. Jing and W. Qi, "Exploring Reciprocal Influence between Individual Shopping Travel and Urban Form: Agent-Based Modeling Approach," *J. Urban Plann. Dev.,* vol. 137, *(4),* pp. 390-401, 2011. Available: https://doi.org/10.1061/(ASCE)UP.1943-5444.0000084. DOI: 10.1061/(ASCE)UP.1943-5444.0000084.

[12] H. Haiyan, W. Yan and Wang Qi (Ryan), "Simulating Urban Population Activities under Extreme Events with Data-Driven Agent-Based Modeling," *Construction Research Congress 2022,* pp. 1125-1134, 2022. Available: https://doi.org/10.1061/9780784483961.118. DOI: 10.1061/9780784483961.118.

[13] K. Feng and N. Lin, "Modeling and analyzing the traffic flow during evacuation in Hurricane Irma (2017)," *Transportation Research Part D: Transport and Environment,* vol. 110, pp. 103412, 2022. Available: https://www.sciencedirect.com/science/article/pii/S1361920922002383. DOI: 10.1016/j.trd.2022.103412.

[14] Y. Wang *et al,* "The impact of electrical hazards from overhead power lines on urban search and rescue operations during extreme flood events," *International Journal of Disaster Risk Reduction,* vol. 104, pp. 104359, 2024. Available: https://www.sciencedirect.com/science/article/pii/S2212420924001213. DOI: 10.1016/j.ijdrr.2024.104359.

[15] Y. Li and W. Ji, "Bayesian-based forecasting of infrastructure restoration progress following extreme events," *International Journal of Disaster Risk Reduction,* pp. 103519, 2022. Available:

https://www.sciencedirect.com/science/article/pii/S2212420922007385. DOI: 10.1016/j.ijdrr.2022.103519.

[16] E. Tate *et al*, "Flood exposure and social vulnerability in the United States," *Nat. Hazards,* vol. 106, *(1),* pp. 435-457, 2021. Available: https://doi.org/10.1007/s11069-020-04470-2. DOI: 10.1007/s11069-020-04470-2.

[17] C. T. Emrich *et al*, "Measuring social equity in flood recovery funding," *Environmental Hazards,* vol. 19, *(3),* pp. 228-250, 2020. Available: https://doi.org/10.1080/17477891.2019.1675578. DOI: 10.1080/17477891.2019.1675578.

[18] S. Dong *et al*, "An integrated physical-social analysis of disrupted access to critical facilities and community service-loss tolerance in urban flooding," *Comput. , Environ. Urban Syst.,* vol. 80, pp. 101443, 2020. Available: https://www.sciencedirect.com/science/article/pii/S019897151930434X. DOI: 10.1016/j.compenvurbsys.2019.101443.

[19] A. Ermagun, V. Smith and F. Janatabadi, "High urban flood risk and no shelter access disproportionally impacts vulnerable communities in the USA," *Communications Earth & Environment,* vol. 5, *(1),* pp. 2, 2024. Available: https://doi.org/10.1038/s43247-023-01165-x. DOI: 10.1038/s43247-023-01165-x.

[20] Y. Li, C. Yang and W. Ji, "Enhanced prediction of highway flood inundation through Bayesian generalized linear geostatistical models," *Advanced Engineering Informatics,* vol. 61, pp. 102451, 2024. Available: https://www.sciencedirect.com/science/article/pii/S1474034624000995. DOI: 10.1016/j.aei.2024.102451.

[21] Y. Wang *et al*, "A Computational Framework for Identifying Safe Evacuation and Rescue Routes in Catastrophic Urban Flooding Environments," *Computing in Civil Engineering 2023,* pp. 136-143, 2024. Available: DOI: 10.1061/9780784485248.017.

[22] FEMA. *Hazus*. Available: https://www.fema.gov/flood-maps/products-tools/hazus.

[23] United States Census Bureau. *Explore Census Data*. Available: https://data.census.gov/.

[24] U.S. Army Corps of Engineers, "Millstone river basin, new Jersey Flood risk management feasibility Study Final feasibility report," Nov. 2016.

[25] CBS New York. *Nightmare In Manville, NJ As Homes And A Business Explode In Ida's Aftermath; Family Grateful To Be Alive*. Available: https://www.cbsnews.com/newyork/news/ida-manville-new-jersey-flood/.

[26] Y. Wang, J. Gong and C. Di, "A building-scale hydrodynamic model for extreme urban flash flooding simulation: A Confluence Area in Raritan River Basin during Hurricane Ida," *ESS Open Archive,* 2022. DOI: 10.1002/essoar.10512267.1.

[27] E. Hunter, "Rartian River Basin Elevation Data. Rutgers University."

[28] Y. Wang and R. Marsooli, "Physical Instability of Individuals Exposed to Storm-Induced Coastal Flooding: Vulnerability of New Yorkers During Hurricane Sandy," *Water Res.,* vol. 57, *(1),* pp.

e2020WR028616, 2021. Available: https://doi.org/10.1029/2020WR028616. DOI: 10.1029/2020WR028616.

[29] J. Xia and J. Gong, "Computer vision based first floor elevation estimation from mobile LiDAR data," *Autom. Constr.,* vol. 159, pp. 105258, 2024. Available: https://www.sciencedirect.com/science/article/pii/S0926580523005186. DOI: 10.1016/j.autcon.2023.105258.

An Integrated Metric for Rapid and Equitable Emergency Rescue During Extreme Floods in Urban Environments

Yitong Li[1*] Yifan Wang[2*] and Jie Gong[3]

[1]Postdoctoral Associate, Department of Civil and Environmental Engineering, Rutgers, The State University of New Jersey; Email: yl2035@soe.rutgers.edu

[2]Research Associate, Department of Civil and Environmental Engineering, Rutgers, The State University of New Jersey; Email: yw922@soe.rutgers.edu

[3]Associate Professor, Department of Civil and Environmental Engineering, Rutgers, The State University of New Jersey; Email: jg931@soe.rutgers.edu (corresponding author)

*These authors contributed equally to this work.